of water vapor at height y (abs. atm); r_1, μ, α, β, latent heat of evaporation referred to specific heat of vapor (deg), heat of hydration per kg of water referred to specific heat of vapor (deg), heat-transfer coefficient (kcal/m²·h·deg), and mass-transfer coefficient (kg/m²·h·atm).

LITERATURE CITED

1. G. I. Shishkin, V. F. Volkov, V. F. Egolaeva, and V. V. Ukhlov, "Sectionalization of fluidized beds," Inzh.-Fiz. Zh., 29, No. 3 (1975).
2. V. F. Volkov, V. M. Pavlov, et al., Khim. Prom-st, No. 6 (1966).
3. V. F. Volkov, I. I. Shishko, and L. V. Khokhlova, in: Heat and Mass Transfer [in Russian], Vol. 5, Minsk (1968).
4. O. M. Todes, Yu. Ya. Kaganovich, et al., Fluidized-Bed Solution Evaporation [in Russian], Metallurgiya, Moscow (1973).

AXIAL DISPLACEMENT OF SOLID PHASE IN A CONTAINED FLUIDIZED BED

Yu. S. Teplitskii and A. I. Tamarin

UDC 532.546

Thermal labeling has been used to examine axial heat transport (solid-phase transport) in a fluidized bed with low-volume packing for columns of diameters 15, 30, and 70 cm.

Many low-volume retaining systems [8, 9, 11, 12] such as horizontal grids, perforated plates, gridded cylinders, and wire spirals can adversely affect the displacement of the solid material, because they break up the gas bubbles and thus reduce the rise speed considerably [2, 17].

If such devices are to be used to advantage, especially when rapid particle motion is to be combined with high heat-transfer performance, it is necessary to know the laws governing the motion of the solid phase and the heat, particularly as regards effects of system scale.

The vertical particle movement in a free bed is similar to that in a contained one, in that there is circulation due to particle transport in the surfaces of rising bubbles, together with exchange of particles between the surfaces of bubbles by diffusion. When these bubbles flow around fixed elements in the containment, there is additional transfer, particularly due to displacement of particles from the surface of the bubbles.

Therefore, the transport of the solid (heat) in a fluidized system can be considered as a combination of convection and diffusion [10]. The available immobile packing accentuates the diffusion and tends to suppress the circulation. Measurements show that the gas nonuniformities in such a system are much smaller in scale and more uniformly distributed in space [2, 17], while the particle motion is close to the diffusion type [1, 18]. It would seem [13] that the radial displacement in such a system is extremely close to diffusion type.

As all the particles remain within the system for times much exceeding the time corresponding to descent through the bed, the transport may be considered of diffusion type and

TABLE 1. Characteristics of Materials

Powder material	d_{av}, mm	u_0, cm/sec	ρ_4, kg/m³	Symbol in text
Quartz sand	0,24	5	2650	Q.1
Quartz sand	0,6	20	2540	Q.2
Silica gel	0,2	2	1100	S

A. V. Lykov Institute of Heat and Mass Transfer, Academy of Sciences of the Belorussian SSR, Minsk.

Translated from Inzhenerno-Fizicheskii Zhurnal, Vol. 33, No. 4, pp. 603-610, October, 1977. Original article submitted March 11, 1977.

0022-0841/77/3304-1148$07.50

TABLE 2. Characteristics of Contained Fluidized Beds

Containment	l_p, cm	ε_p	Solid particles (see Table 1)	D_c, cm	H_0, cm
Cylindrical spirals, 50 mm diameter; wire diameter 2.5 mm	3,06	0,980	Q.1 Q.2 S	30 30 30	90; 130; 150 40; 75; 100 50; 90;
Cylindrical spirals 25 mm diameter; wire diameter 1 mm	0,57	0,958	Q.1	30 15	25; 50 30; 60
Cylindrical spirals 10 mm diameter; wire diamter 1 mm	0,35	0,933	Q.1	15	25
Horizontal grids (clear area of cell 8×8 wire diameter 1.3 mm, vertical pitch 4 cm)	3,7	0,991	Q.1 S	30 70 30	70; 100 50; 90; 150 30; 60; 80
Stacks of perforated plates, 5.5. cm height, inclined in opposite direction, hole sizes 6 and 12 mm	2,5	0,976	Q.1 Q.2 S	30 30 30	60; 100 45; 70; 100 60; 85;

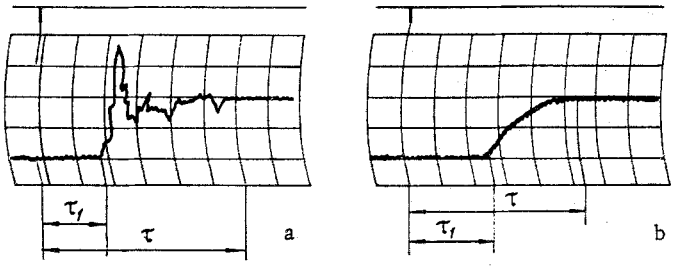

Fig. 1. Characteristic form of signal from thermocouple at grid in column: a) free bed, H_0 = 45 cm, $u - u_0$ = 35 cm/sec; material Q.1; b) spirals of diameter 50 mm [16]; H_0 = 65 cm, $u - u_0$ = 46 cm/sec; material Q.1.

as described by some effective diffusion coefficient. If there are any fast processes whose time scales are comparable with $\bar{\tau}_C$, one has to consider the details of the circulation in addition [14].

It is therefore clear that one needs to know the details of the circulation and the diffusion aspect in such a contained fluidized system.

Very little has been published on particle motion in fluidized beds with such elements, and much of the evidence is conflicting; the rates of transport of heat and solid in such beds have [1, 3-5, 9, 11] been evaluated in terms of an axial diffusion coefficient for the heat (solid phase) $\hat{K}_z$; some data [1, 9] indicate that $\hat{K}_z$ is independent of H_0, whereas those of [11] indicate that $\hat{K}_z$ is very substantially dependent on the initial bed depth. Closely spaced retainers give $\hat{K}_z$ lower than those for widely spaced ones [3, 5, 11]. On the other hand, the converse relationship has been reported [9]. It is stated [11] that the mixing increases as the speed at onset of fluidization falls, whereas in [1] it is stated that $\hat{K}_z$ increases with the particle size. Cinephotography in an equipment with a transparent wall has shown [8] that the retainers (horizontal wire grids) reduce the rate of descent of the material by a factor of 5-10. A point here is that most of these results have been obtained for small systems ($D_c \leqslant 30$ cm, $H_0 \leqslant 60$ cm).

We have obtained quantitative results on the circulation speeds of particles and of the effective axial diffusion coefficient for the solid phase, both in relation to the scale of the system.

Tables 1 and 2 give the working conditions; we used heat labeling [6], with the heated particles recorded by thermocouples (one at the bottom of the bed and the other at about half height). Both were at the axis of the column. The thermocouple signals were recorded with an N327-3 chart recorder. Rapid addition of a small batch of particles heated in a muffle

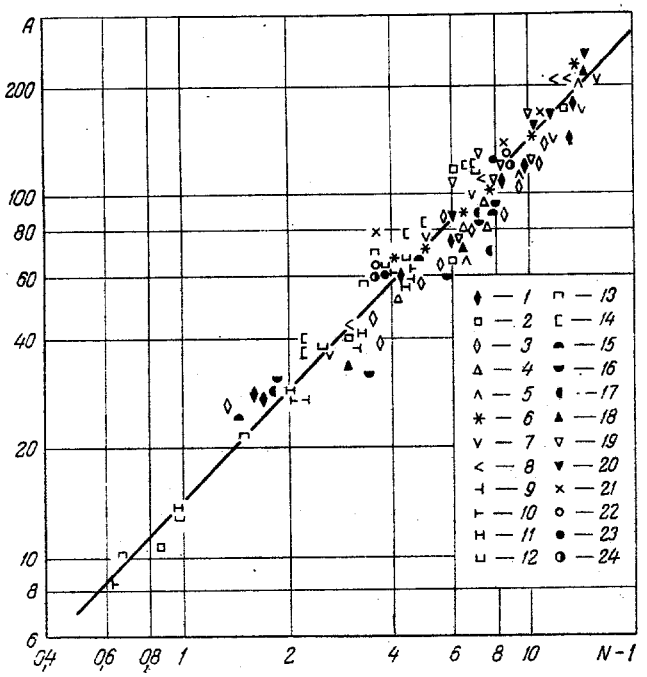

Fig. 2

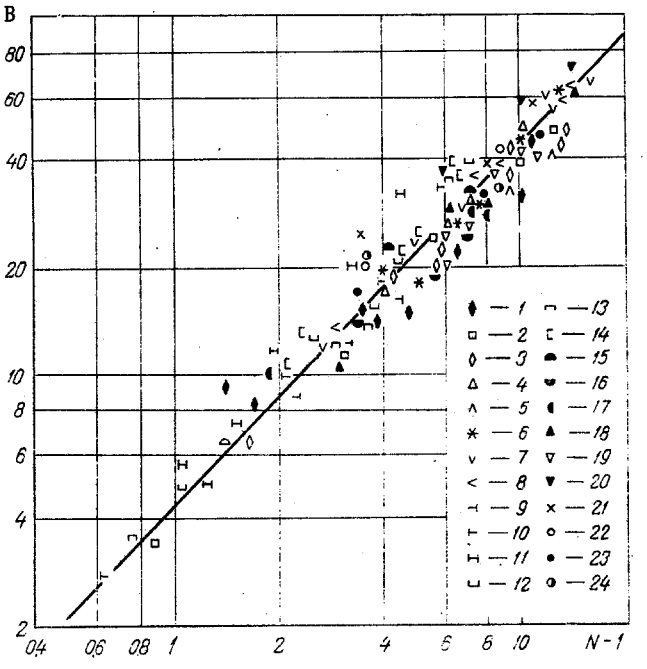

Fig. 3

Fig. 2. Relationship between $w_d^{max}Re^{0.4}(\rho_p/\rho_g)^{0.5}[(l_p + l_0)/l_p]/u_0Fr^{*0.17}$ (A) and the dimensionless excess gas speed N − 1: 1-4) l_p = 3.06 cm (H_0 = 65, 90, 130, 150 cm); 5, 6) l_p = 0.57 cm (H_0 = 25, 50 cm); 7, 8) l_p = 2.5 cm (H_0 = 60, 100 cm); 9-11) l_p = 3.06 cm (H_0 = 40, 75, 100 cm); 12-14) l_p = 2.5 cm (H_0 = 45, 70, 100 cm); 15-17) l_p = 3.7 cm (H_0 = 50, 90, 150 cm); 18, 19) l_p = 0.57 cm (H_0 = 25, 50 cm); 20) l_p = 0.345 cm (H_0 = 30 cm); 21, 22) l_p = 3.06 cm (H_0 = 50, 90 cm); 23, 24) l_p = 2.5 cm (H_0 = 60, 85 cm). Materials: 1-8 and 15-20) Q.1; 9-14) Q.2; 21-24) S (Table 1); Q.1 and Q.2) quartz sand of average diameters 0.24 and 0.6 mm, respectively; S) silica gel, average diameter 0.19 mm. Columns: 1-14, 21-24) D_c = 30 cm; 15-17) D_c = 70 cm; 18-20) D_c = 15 cm.

Fig. 3. Relationship of $w_dRe^{0.4}(\rho_p/\rho_g)^{0.5}[(l_p + l_0)/l_p](H_0/D_c)^{-0.3}/u_0Fr^{0.1}$ (B) to N − 1; see Fig. 2 for symbols.

furnace (less than 1% of the bed mass) produced an instantaneous planar heat source at the upper end of the bed. This instant was recorded with the chart recorder time marker.

Figure 1b shows the characteristic form of the signal from the thermocouple at the bottom of the bed (4 cm above the gas distributor). For comparison, Fig. 1a shows the similar signal for a free bed. The main difference between Figs. 1a and b is the absence of sharp bursts in the contained case (Fig. 1b). The containment has a smoothing effect on the system and eliminates marked fluctuations in the circulation speed [7, 18]. Parts a and b of Fig. 1 also indicate the characteristic delay τ_1 and the mean time of arrival τ for the pulse at a given point.

The speed of the descent was calculated from the following equations: maximum descent speed

$$w_d^{max} = H/\tau_1 \quad (1)$$

average descent speed

$$w_d = H/\tau. \quad (2)$$

The bed depth was determined visually. If necessary (e.g., at high speeds) a correction was applied via the theoretical formulas

$$\hat{p} - 1 = 26\,Re^{-0.4}(\rho_p/\rho_g)^{-0.5}Fr_1^{*0.7}. \quad (3)$$

In each case, w_d^{max} and w_d were determined as the means of six appropriate values in six independent runs.

The results were processed by least squares and the π-theorem in the method of dimensions [15]. The following generalized regression lines were derived:

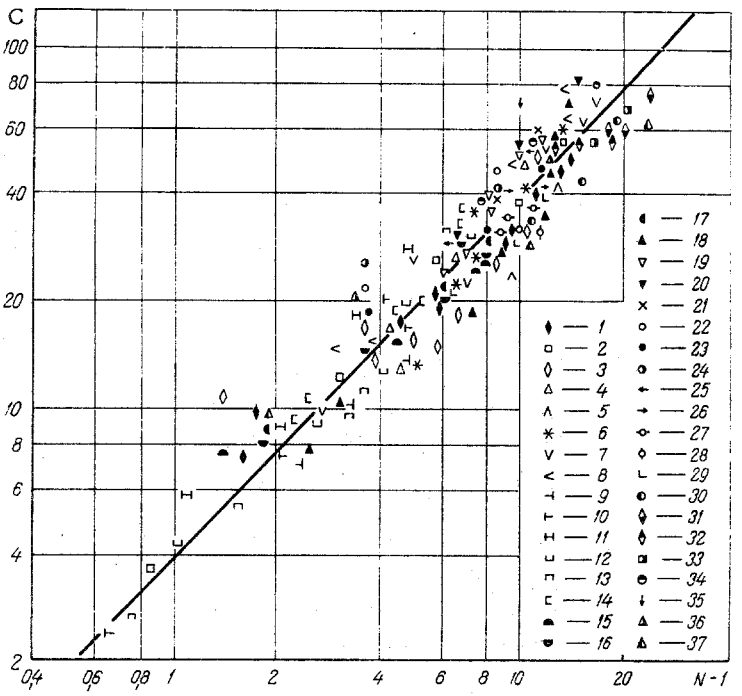

Fig. 4. Relation of $(\hat{K}_z Re^{0.4}/u_0 H_0)(\rho_p/\rho_g)^{0.5}[(l_p + l_0)/l_p]/Fr^{*0.17}$ (C) to N − 1: 1-24) see Fig. 2 for symbols; 25-35) [11]; 25) l_p = 3.06 cm (H_0 = 30 cm); 26-28) l_p = 0.57 cm (H_0 = 30, 45, 60 cm); 29) l_p = 2.45 cm (H_0 = 45 cm); 30) l_p = 3.06 cm (H_0 = 30 cm); 31, 32) l_p = 0.57 cm (H_0 = 30, 45 cm); 33, 34) l_p = 2.45 cm (H_0 = 30, 60 cm); 35) l_p = 0.345 cm (H_0 = 30 cm); 36, 37) [5]; $l_p \cong$ 0.6; 2.4 cm ($H_0 \cong$ 45 cm). Materials: 25-29) quartz sand, average diameter 0.23 mm; 30-35) silica gel, 0.19 mm; 36 and 37) FCC cracking catalyst, d = 0.065 mm. Columns: 25-35) D_c = 30 cm; 36 and 37) D_c = 8 cm. Packing: 25-28, 30-32, and 35) wire spirals [16]; 29, 33, and 34) perforated plates; 36 and 37) gridded cylinders.

$$w_d/(u-u_0) = 15.5\,Re^{-0.4}Fr^{*0.17}\left(\frac{l_p}{l_p+l_0}\right)\left(\frac{\rho_p}{\rho_g}\right)^{-0.5}, \quad (4)$$

$$w_d/(u-u_0) = 4.2\,Re^{-0.4}Fr^{0.1}\left(\frac{l_p}{l_p+l_0}\right)\left(\frac{H_0}{D_c}\right)^{0.3}\left(\frac{\rho_p}{\rho_g}\right)^{-0.5}, \quad (5)$$

which are shown along with the observed points in Figs. 2 and 3. The coefficients of variation about (4) and (5) are approximately identical at 20%.

These equations are best compared with our analogous results for a free bed:

$$w_d^{max}/(u-u_0) = 0.16\,Re^{-0.2}Fr^{*-0.25}, \quad w_d/(u-u_0) = 0.056\,Re^{-0.2}Fr^{-0.22}. \quad (6), (7)$$

These equations allow one to determine $\beta = w_d^{max}/w_d - 1$, which characterizes the rate of particle exchange between the surfaces of bubbles and the descending flows (β = 2.7 for a contained bed and β = 1.85 for a free bed).

A contained bed therefore has diffusion as a much more prominent mechanism (turbulent mixing due to the eddies).

The particle speed in a contained bed varies more rapidly with $(u - u_0)$ than does that in a free bed; the circulation rate in a contained system is always less than that in the corresponding free bed, although the two tend to become more similar as $u - u_0$ increases. The particle speed is more dependent on Re and ρ_p in a contained bed. Finally, the containment reduces the descent speed, since it constitutes a geometrical obstacle $l_p/(l_p + l_0)$ to the particle motion.

The value for w_d allows us to determine $\bar{\tau}_C = H/w_d$; if $\tau < \bar{\tau}_C$, it is also necessary to consider the transport of the solid by circulation.

One is justified in using an axial diffusion coefficient for $\tau > \bar{\tau}_C$, and then this is given by the formula

$$\hat{K}_z = H^2/2\tau. \tag{8}$$

The data were analyzed in the way used for the circulation speeds; the generalized regression equation is

$$\hat{K}_z/(u-u_0)H_0 = 3.76\,\mathrm{Re}^{-0.4}\left(\frac{\rho_p}{\rho_g}\right)^{-0.5}\frac{l_p}{l_p+l_0}\,\mathrm{Fr}^{*0.17}. \tag{9}$$

Figure 4 shows the measurements and the curve of (9), as well as the results of [5, 11]. The coefficient of variation for the observed points is 30%, which is quite acceptable for this purpose. Horizontal grids in a column of diameter 30 cm gave a more marked effect from the velocity, $\hat{K}_z \sim (u - u_0)^2$, and these were omitted from the analysis.

We may compare (9) with the analogous one for a free bed

$$\hat{K}_z/(u-u_0)H_0 = 0.1\,\mathrm{Re}^{-0.4}, \quad N > 3. \tag{10}$$

In both cases we find $\hat{K}_z \sim H_0$, which indicates that the axial displacement in in the mixed fraction of a free and contained bed is of circulation type, as is Re. At the same time the material density depends on addition packing of the contained bed. The mixing tends to deteriorate as the density increases.

Finally, we note that (4), (5), and (9), which describe the axial solid or heat transport in the system, apply within the following limits for the parameters: $1100 \leqslant \rho_p \leqslant 2650$ kg/m^3; $8 \leqslant D_c \leqslant 70$ cm; $0.02 \leqslant \mathrm{Re} \leqslant 8$; $0.345 \leqslant l_p \leqslant 3.7$ cm; $30 \leqslant H_0 \leqslant 150$ cm.

These correlations can be utilized in calculating mixing rates and heat transport for industrial fluidized-bed systems.

NOTATION

d, particle diameter; D_c, column diameter; g, acceleration due to gravity; H_0 and H, heights of bed for u_0 and u, respectively; $H/H_0 = \hat{p}$, bed expansion; $l_p = (V_b - V_p)/F_p$, equivalent size of the packing; F_p and V_p, total surface area and packing volume in the bed; V_b, volume of bed; l_0, dimensional parameter ($l_0 = 1.2$ cm); u_0 and u, velocities at the onset of fluidization and in working state, respectively; $N = u/u_0$, fluidization number; $\hat{K}_z$, axial particle diffusion coefficient w_d^{max} and w_d, maximum and mean velocities of downward motion; $\mathrm{Re} = u_0 d/\nu$, critical Reynolds number; $\mathrm{Fr} = (u-u_0)^2/gH_0$, Froude number; $\mathrm{Fr}^* = \mathrm{Fr}H_0/D_c$; $\mathrm{Fr}_1^* = \mathrm{Fr}H_0/(l_p + l_0)$; ρ_p and ρ_g, density of particles and gas, respectively; ν, kinematic viscosity; τ_1 and τ, times of arrival of fast-moving particles and majority of particles at the point of temperature measurement; $\tau_C = H/w_d$; $\varepsilon_p = 1 - V_p/V_b$, packing porosity.

LITERATURE CITED

1. N. V. Kuzichkin, I. P. Mukhlenov, A. T. Bartov, and A. N. Prokopenko, Inzh.-Fiz. Zh., 29, No. 4 (1975).
2. N. V. Kuzichkin, Candidate's Dissertation, Leningrad Technological Institute, Leningrad (1973).
3. V. A. Chumachenko, Candidate's Dissertation, Novosibirsk (1974).
4. S. G. Bashkirova, Candidate's Dissertation, Moscow (1974).
5. K. Kato, K. Imafuko, K. Hattori, and H. Kubota, Kagaku Kogaku, 5, No. 1 (1967).
6. V. A. Borodulya and A. I. Tamarin, Inzh.-Fiz. Zh., 5, No. 11 (1962).
7. O. M. Todes, A. K. Bondareva, and M. B. Grinbaum, Khim. Prom-st., No. 6 (1966).
8. L. Massimilla and J. M. Westwater, AIChE J., 6, 134 (1960).
9. W. K. Kang and G. L. Osberg, Can. J. Chem. Eng., 44, 142 (1966).
10. M. M. Rozenberg, M. B. Kats, and L. I. Kheifets, Teor. Osn. Khim. Tekhnol., 8, No. 6 (1974).
11. R. R. Khasanov, Candidate's Dissertation, Institute of Heat and Mass Transfer, Academy of Sciences of the Belorussian SSR, Minsk (1974).
12. J. F. Davidson and D. Harrison (editors), Fluidization, Cambridge University Press (1963).
13. V. M. Pakhaluev, Candidate's Dissertation, Ural Polytechnic Institute, Sverdkovsk (1969).
14. V. D. Meshcheryakov and V. S. Sheplev, in: Proceedings of the Second Soviet–French Seminar on Mathematical Simulation of Catalytic Processes and Reactors [in Russian], Novosibirsk (1976), p. 123.

15. L. I. Sedov, Similarity and Dimensional Methods in Mechanics [in Russian], Nauka (1965).
16. A. I. Tamarin and V. D. Dunskii, Inventor's Certificate No. 24246, Byull. Izobr., No. 15 (1969).
17. W. H. Park, W. K. Kang, C. E. Capes, and G. L. Osberg, Chem. Eng. Sci., 24, 851 (1969).
18. E. N. Prozorov, Khim. Prom-st, No. 11 (1975).

EXPERIMENTAL INVESTIGATION OF TUBE FLOW OF A GAS-PARTICLE MIXTURE

V. V. Zlobin

UDC 532.529

The results of an experimental investigation of the velocity distribution and the discrete-phase mass flow distribution in an ascending gas-particle tube flow are presented and partially generalized.

In two-phase flow the conditions of jet formation, determined by the characteristics of the accelerating device, have a much greater influence on subsequent flow development than in the case of single-phase flow. The simplest effective accelerating device is a length of round tubing. In this case the characteristics of the tube flow enter into the initial jet flow conditions. The existing publications on the tube flow of gas-particle mixtures are mainly concerned with questions of heat transfer and pneumatic transport, while the direct study of the mechanics of fine-dispersion flows has been held back by the lack of suitable measuring techniques. Recently developed methods of probing flows of the gas-particle type with lasers [1, 2] have opened up prospects of obtaining the necessary information.

The most important factor influencing the distribution of the discrete phase in a two-phase jet system is the phase slip velocity produced by the accelerating device. It is impossible to exclude the effect of the nonuniformity of the discrete-phase distribution, although it is difficult to estimate. Certain information concerning the distribution of particle concentration and mass flow on the particle size range of interest is provided by Soo in [3-5], who noted a maximum of the particle mass flow distribution on the flow axis. The particle velocity data were obtained by conversion of the results for the particle concentration and mass flow and it was noted that the mean particle velocity lagged behind the mean gas velocity.

We have studied the phase velocity distribution and the discrete-phase mass flow distribution in an ascending tube flow with reference to the particle size of the discrete phase, the velocity of the carrier phase, and the tube diameter. The stainless-steel tubes were 0.9 m long and had the following inside diameters: 7.8; 12.2; 15.6; and 25.8 mm. As the discrete phase we used narrow-fraction electrocorundum powders with a mean mass particle size of 23, 32, 70, or 88 μ and density of 3.9 g/cm^3. The carrier phase was air at 15-20°C. The air velocity was varied on the range 10-90 m/sec and the Reynolds number, based on the mean gas velocity, on the range from $5\cdot10^3$ to 10^5. In order to eliminate as far as possible the reaction of the discrete phase on the gas-phase velocity field, in almost all cases the mass flow concentration $\varkappa$ was kept at 0.3 or less [6], except at $\bar{v} \sim 10$ m/sec, when $\varkappa$ reached values of 0.8-1.0 kg•h/kg•h. The distribution of the discrete phase and its velocity were measured by optical laser methods at a distance of 3 mm from the tube exit. In order to exclude the possibility of electrization of the particles [7], the apparatus was grounded. A more detailed description of the measurements and the apparatus may be found in [8].

Under the experimental conditions (isothermal flow, $\varkappa \to 0$), steady-state flow of the two-phase system was primarily determined by forces of a hydrodynamic nature and a system of criteria can be constructed from the ratio of mean mass particle size to tube diameter d_s/D, the Reynolds number $Re = \bar{v}D/\nu$, and the particle-gas density ratio ρ_p/ρ. In this case the adhesion properties of the particle—tube surface interaction can be defined in terms of the

Institute of Thermophysics and Electrophysics, Academy of Sciences of the Estonian SSR, Tallin. Translated from Inzhenerno-Fizicheskii Zhurnal, Vol. 33, No. 4, pp. 611-616, October, 1977. Original article submitted November 22, 1976.

0022-0841/77/3304-1153$07.50